

## Search for the $A_1$ in $\tau \rightarrow \nu_\tau \rho \pi$

D. A. Geffen and Warren J. Wilson

*University of Minnesota, School of Physics and Astronomy, Minneapolis, Minnesota 55455*

(Received 8 May 1978)

Within the context of current algebra, we analyze the possibility of observing the elusive  $A_1$  meson ( $J^{PC} = 1^{++}$ ) in the heavy-lepton decay  $\tau^\pm \rightarrow \nu_\tau \rho^0 \pi^\pm$ . In our model the form factors for the decay amplitude are then completely determined in terms of the  $A_1$  mass and width so that we are able to predict both the branching ratio and  $\rho\pi$  mass spectrum for this decay. We find that the data are compatible with a wide range of  $A_1$  parameters including the possibility that there is no  $A_1$  contribution at all to this decay mode. Only a modest increase in experimental precision, however, would provide a stringent test of the current-algebra model and, if successful, yield an accurate determination of the parameters of the  $A_1$ .

### I. INTRODUCTION

As has been noted by several authors,<sup>1</sup> the recently observed heavy lepton  $\tau^\pm$  should have some interesting semihadronic decay modes. One mode of particular interest is the decay

$$\tau^\pm \rightarrow \nu_\tau \rho^0 \pi^\pm \rightarrow \nu_\tau \pi^* \pi^- \pi^\pm, \quad (1)$$

where we expect the  $\rho\pi$  system to exhibit the resonant structure of the elusive  $A_1$  meson ( $J^{PC} = 1^{++}$ ). To say the least, the attempts of meson spectroscopists to observe the  $A_1$  in purely hadronic processes have been fraught with difficulties.<sup>2</sup> Recent phenomenological analyses<sup>3</sup> of hadronic collisions have been more encouraging although they tend to favor an  $A_1$  of both larger mass and width than those expected from either quark or current-algebra models. Very recently, stronger evidence for  $A_1$  production has been reported by various groups. We cite, for example, the published report of Gavillet *et al.*,<sup>4</sup> who find an  $A_1$  bump in  $K^- p \rightarrow \Sigma^- \pi^- \pi^+ \pi^+$  (backward production). They require for a fit to their  $3\pi$  mass spectrum an  $A_1$  with  $M_A = 1.041 \pm 0.013$  GeV and  $\Gamma_A = 230 \pm 50$  MeV. On the face of it, this seems like a very large width for so small an  $A_1$  mass but it must be remembered that the  $A_1$  decay parameters can be quite distorted in hadronic production processes.

In this paper we return to the current-algebra models of a decade ago and apply them to an analysis of reaction (1). Using current-algebra sum rules previously derived by several authors,<sup>5</sup> including one of us (D. G.), we find that we are able to completely describe reaction (1) in terms of known constants and two free parameters, which we can take to be  $M_A$  and  $\Gamma_A$ , the mass and the decay width of the  $A_1$ . (In our analysis the case of a nonexistent  $A_1$  corresponds to the  $\Gamma_A \rightarrow 0$  limit.)

Measurements of the branching ratio and  $\rho\pi$  mass spectrum of reaction (1) are now available but of still limited statistical accuracy. Consequently, while in principle this information will provide a stringent test of the current-algebra predictions and the existence of the  $A_1$ , the present data can only provide some constraints on  $M_A$  and  $\Gamma_A$ , but, as we shall show, *do not yet establish the existence of the  $A_1$ .*

In the next section we present the current-algebra calculations relevant to reaction (1). In Sec. III, we compare our current-algebra results with the data from SLAC and DESY. Finally, in Sec. IV we give a short summary and discuss our results.

### II. CURRENT-ALGEBRA RESULTS

We begin by assuming that the interaction which produces reaction (1) is given by<sup>6</sup>

$$\frac{G_F}{\sqrt{2}} \bar{\nu}_\tau \gamma_\mu (1 - \gamma_5) \tau A^\mu, \quad (2)$$

where  $A_\mu$  is the hadronic weak axial-vector current. The matrix element of interest is just

$$\langle \pi^a(q), \rho^b(p, \epsilon_\rho) | iA_\mu^c | 0 \rangle = i \epsilon_{abc} F_\mu, \quad (3)$$

where  $a$ ,  $b$ , and  $c$  are isospin indices.  $q$  is the momentum of the  $\pi$ ; and  $p$  and  $\epsilon_\rho$  are the momentum and polarization of the  $\rho$ . The most general Lorentz-covariant form of  $F_\mu$  is

$$F_\mu = \epsilon_{\rho\mu} F_0 - (\epsilon_\rho q)(p - q)_\mu F_+ - (\epsilon_\rho q)(p + q)_\mu F_- . \quad (4)$$

We take the  $F_i$  to be functions of  $q^2$  and  $k^2$ ,  $k = p + q$ . After some mildly tedious algebra we find that the differential decay rate can be written in the form

$$\begin{aligned} \frac{d\Gamma}{d(k^2)^{1/2}} &= \frac{G_F^2}{4m_\tau^3} \left(\frac{1}{2\pi}\right)^3 I(k^2), \\ I(k^2) &= \frac{\lambda(k^2)}{(k^2)^{1/2}} (m_\tau^2 - k^2)^2 \\ &\times \left[ \left(\frac{m_\tau^2 + 2k^2}{3k^2}\right) \left( |G_1|^2 + \frac{m_\rho^2}{2k^2} |G_2|^2 \right) \right. \\ &\quad \left. + \frac{m_\tau^2}{8m_\rho^2} \left(\frac{\lambda(k^2)}{k^2}\right)^2 |G_3|^2 \right], \end{aligned} \quad (5)$$

with

$$\begin{aligned} G_1 &= F_0, \\ G_2 &= \frac{k^2 + m_\rho^2 - m_\tau^2}{2m_\rho^2} F_0 - \frac{\lambda(k^2)^2}{2m_\rho^2} F_+, \\ G_3 &= F_0 - (m_\rho^2 - m_\tau^2) F_+ - k^2 F_-. \end{aligned} \quad (6)$$

In Eqs. (5) and (6)  $(k^2)^{1/2}$  is the invariant mass of the  $\rho\pi$  system; and  $\lambda(k^2) = [(k^2 + m_\rho^2 - m_\tau^2)^2 - 4k^2 m_\rho^2]^{1/2}$ .  $\lambda(k^2)/2(k^2)^{1/2}$  is the  $\rho$  momentum in the  $\rho\pi$  rest frame. We have assumed here that the  $\tau$  neutrino is massless.  $G_3$  represents the contribution from the  $J^{PC} = 0^{-+}$  part of the axial-vector current, while  $G_1$  and  $G_2$  measure the  $J^{PC} = 1^{++}$  parts. Thus,  $G_3$  will contain a pion pole, and  $G_1$  and  $G_2$  will contain  $A_1$  poles.

The current-algebra model we use to obtain  $F_\pm$ ,  $F_0$  assumes that the  $F_\pm$  are dominated by their lowest-mass poles,  $A_1$  and  $\pi$  and that  $k^\mu F_\mu$  is given by the pion pole according to partial conservation of axial-vector current (PCAC). We further assume that  $F_0$  can be extrapolated, with negligible change, to zero pion mass. It then follows that, in addition to the  $A_1$  pole, we must expect  $F_0(k^2)$  to have contributions from higher-mass  $1^{++}$  states, which we approximate by a constant. These assumptions

lead to the expressions for  $F_\mu$ ,

$$\begin{aligned} F_+(k^2) &= -F_A g_{A\rho\pi} / D_A(k^2), \\ F_-(k^2) &= -2\gamma_{\rho\pi\tau} F_\tau / (m_\tau^2 - k^2) \\ &\quad + \left(\frac{F_A}{M_A^2}\right) \frac{(M_A^2 - m_\rho^2) f_{A\rho\pi} + (m_\rho^2 - m_\tau^2) g_{A\rho\pi}}{D_A(k^2)}, \\ F_0(k^2) &= C_0 + F_A f_{A\rho\pi} (M_A^2 - m_\rho^2) / D_A(k^2). \end{aligned} \quad (7)$$

The various coupling constants in Eq. (7) are given in Table I.  $D_A^{-1}(k^2)$  is the  $A_1$  propagator.  $C_0$  is the constant approximating the higher-mass  $1^{++}$  contributions to  $F_0$ . The PCAC condition that  $k^\mu F_\mu = \langle \pi\rho | \partial^\mu A_\mu | 0 \rangle$  is dominated by the pion pole requires

$$\begin{aligned} C_0 &= 2\gamma_{\rho\pi\tau} F_\tau \\ &\quad - \left(\frac{F_A}{M_A^2}\right) [(M_A^2 - m_\rho^2) f_{A\rho\pi} + (m_\rho^2 - m_\tau^2) g_{A\rho\pi}]. \end{aligned} \quad (8)$$

Finally, the soft-pion limit  $q \rightarrow 0$  of  $F_\mu$  implies

$$F_0(m_\rho^2) = F_\rho / F_\tau \quad (9)$$

if we can neglect any change in  $F_0$  in extrapolating it from  $q^2 = m_\tau^2$  to  $q^2 = 0$ . Equations (7), (8), and (9) yield the well known current-algebra sum rule<sup>5</sup>

$$f_{A\rho\pi} - g_{A\rho\pi} = \left(1 - \frac{2\gamma_{\rho\pi\tau} F_\tau^2}{F_\rho}\right) \frac{M_A^2}{m_\rho^2} \frac{F_\rho}{F_A F_\tau}. \quad (10)$$

The first factor in Eq. (10), which we call  $\delta$ , can be determined from the experimental values given in Table I:

$$\delta = 1 - 2\gamma_{\rho\pi\tau} F_\tau^2 / F_\rho = 0.06 \pm 0.06. \quad (11)$$

TABLE I. Definitions of the coupling constants used in our analysis. The experimental values listed in the right-hand column are the values gotten by considering the following measurements: (a)  $\Gamma(\rho \rightarrow \pi\pi)$ , (b)  $\Gamma(\pi \rightarrow \mu\nu)$ , and (c)  $\Gamma(\rho^0 \rightarrow e^+e^-)$ . The experimental inputs are from Ref. 7.

Coupling constant	Definition	Experiment
$f_{A\rho\pi}$	$\langle \rho^a(p, \epsilon_\rho)   j_\tau^b   A_1^c(k, \epsilon_A) \rangle$	...
$g_{A\rho\pi}$	$= i\epsilon_{abc} [(M_A^2 - m_\rho^2) f_{A\rho\pi} (-\epsilon_\mu^\rho \epsilon_A^\mu) - 2g_{A\rho\pi} (\epsilon_\rho k) (\epsilon_A p)]$	...
$\gamma_{\rho\pi\tau}$	$\langle \pi^a(q)   j_\tau^b   \rho^c(p, \epsilon) \rangle = 2i\epsilon_{abc} (\epsilon q) \gamma_{\rho\pi\tau}$	$6.05 \pm 0.06$ (a)
$F_\tau$	$\langle 0   iA_\mu^a   \pi^b(q) \rangle = \delta_{ab} F_\tau q_\mu$	$0.094 \pm 0.001$ GeV (b)
$F_\rho$	$\langle 0   \mathbf{V}_\mu^a   \rho^b(p, \epsilon) \rangle = \delta_{ab} F_\rho \epsilon_\mu$	$0.113 \pm 0.007$ GeV <sup>2</sup> (c)
$F_A$	$\langle 0   A_\mu^a   A_1^b(k, \epsilon) \rangle = \delta_{ab} F_A \epsilon_\mu$	...

In a similar manner, a second sum rule is obtained by interchanging the roles of the  $\rho$  and  $A_1$  and treating the matrix element  $\langle \pi | V_\mu | A_1 \rangle$  to obtain

$$f_{A\rho\pi} + g_{A\rho\pi} = \frac{M_\rho^2}{M_{A_1}^2} \left( \frac{F_{A_1}}{F_\rho F_\pi} \right). \quad (12)$$

Combining the two sum rules and Eqs. (6) and (7) yields for the  $G_i$

$$\begin{aligned} G_1 &= \frac{F_\rho}{F_\pi} \left( 1 + \frac{k^2 - m_\rho^2}{D_A(k^2)} K f_{A\rho\pi} \right), \\ G_2 &= \frac{F_\rho}{F_\pi} \left[ \frac{k^2 + m_\rho^2}{2m_\rho^2} \left( 1 + \frac{k^2 - m_\rho^2}{D_A(k^2)} K f_{A\rho\pi} \right) \right. \\ &\quad \left. + \frac{(k^2 - m_\rho^2)^2}{2m_\rho^2 D_A(k^2)} K g_{A\rho\pi} \right], \\ G_3 &= \frac{F_\rho}{F_\pi} (1 - \delta) \frac{m_\pi^2}{m_\pi^2 - k^2}, \end{aligned} \quad (13)$$

with

$$K \equiv F_{A_1} F_\pi / F_\rho = F_\pi^2 (f_{A\rho\pi} + g_{A\rho\pi}) M_{A_1}^2 / m_\rho^2$$

and

$$f_{A\rho\pi} = (g_{A\rho\pi}^2 + \delta / F_\pi^2)^{1/2}.$$

Note that  $G_3$  is negligible compared to  $G_1$  and  $G_2$  since  $k^2 \gg m_\pi^2$  in reaction (1).

The relative size of the  $A_1$  contribution to the  $G_1$  in Eq. (13) is controlled by the factors  $K f_{A\rho\pi}$  and  $K g_{A\rho\pi}$ . By its definition  $K$  is related to the ratio  $F_{A_1}/F_\rho$ . This ratio is usually assumed to be  $\sim 1$ . If this is the case then we do *not* expect the  $A_1$  contribution to dominate over the non-resonant contribution. Thus, if the  $A_1$  resonance is present in the data we should expect to find it along with some non-negligible "background."

Our expressions for the  $G_i$  along with the sum rules (10) and (12) are the simplest that can be constructed compatible with current algebra. However, higher-mass  $1^{++}$  contributions to  $F_0$  and high-mass  $1^{--}$  contributions to its counterpart in  $\langle \pi | V_\mu | A_1 \rangle$  turn out to be substantial. It is therefore conceivable that similar contributions must be included in  $F_\pm$  as well. We expect these higher-mass contributions to couple less strongly to  $F_\pm$  so that our neglect of such terms in  $F_\pm$  remains the most reasonable assumption to make at this stage. The reader should keep in mind, therefore, that our results come from the simplest current-algebra model but not necessarily the correct one.

So far we have assumed the existence of a low-lying axial-vector meson that couples significantly to the  $\rho\pi$  channel. We now need to consider, as a basis for comparison, the case when the  $A_1$  is not present or decouples from  $\rho\pi$ . We still im-

pose the current-algebra requirements of PCAC and Eq. (9) to Eq. (3). For simplicity, we can take  $\delta = 0$  and then  $F_0$ ,  $F_\pm$  can be obtained from Eqs. (7) and (8) by setting  $f_{A\rho\pi} = g_{A\rho\pi} = 0$  ( $\delta = 0$  implies  $2\gamma_{\rho\pi\pi} F_\pi = F_\rho / F_\pi$ ).  $F_+$  vanishes,  $F_-$  is given by the pion pole, and  $F_0 = F_\rho / F_\pi$  is constant. This represents the simplest choice for the  $F_\mu$  consistent with current-algebra constraints and the notion that only  $F_0$  gets important contributions from higher-mass  $1^{++}$  states. The  $G_i$  become

$$\begin{aligned} G_1 &= F_\rho / F_\pi, \\ G_2 &= \frac{k^2 + m_\rho^2}{2m_\rho^2} F_\rho / F_\pi, \\ G_3 &\approx 0. \end{aligned} \quad (13')$$

When  $\delta$  is nonzero, we have  $F_+$  proportional to  $\delta$ , and it can easily be neglected. Reaction (1) is now dominated by  $F_0 = F_\rho / F_\pi$ . This implies that even in the absence of an  $A_1$  contribution, the  $J^{PC} = 1^{++}$  channel is still the dominant one.

Note that the  $G_i$  in Eq. (13') are now completely determined by experiment so they give both the rate (or branching ratio) and the spectrum.

Finally, to compare our predictions with experiment, we need an expression for  $D_A^{-1}(k^2)$ , the  $A_1$  propagator. For large  $A_1$  widths, the form for  $D_A(k^2)$  can differ considerably from a simple Breit-Wigner form. In general  $D_A(k^2)$  will be model dependent.<sup>8</sup> For our purposes, however, it is sufficient to choose a simple form,

$$D_A(k^2) = M_{A_1}^2 - k^2 - iM_{A_1} \Gamma_A(k^2),$$

with

$$\begin{aligned} \Gamma_A(M_{A_1}^2) &\equiv \Gamma_A^0 = \frac{\lambda(M_{A_1}^2)}{12\pi} \frac{(M_{A_1}^2 - m_\rho^2)^2}{M_{A_1}^3} \\ &\quad \times \left\{ f_{A\rho\pi}^2 + \frac{m_\rho^2}{2M_{A_1}^2} \left[ \frac{M_{A_1}^2 + m_\rho^2}{2m_\rho^2} f_{A\rho\pi} \right. \right. \\ &\quad \left. \left. + \frac{M_{A_1}^2 - m_\rho^2}{2m_\rho^2} g_{A\rho\pi} \right]^2 \right\} \end{aligned} \quad (14)$$

with  $\lambda(M_{A_1}^2) = [(M_{A_1}^2 + m_\rho^2 - m_\pi^2)^2 - 4M_{A_1}^2 m_\rho^2]^{1/2}$ . A  $k^2$  dependence for  $\Gamma_A$  is required by unitarity. We find that our results are insensitive to the details of  $\Gamma_A(k^2)$  provided that (1) it has a threshold factor in the proper position i.e., at  $k^2 = (m_\rho + m_\pi)^2$  and (2) it obeys the following integral condition

$$\frac{1}{\pi} \int dk^2 \text{Im}[M_{A_1}^2 - k^2 - iM_{A_1} \Gamma_A(k^2)]^{-1} = 1. \quad (15)$$

We have chosen to use the form

$$\Gamma_A(k^2) = \Gamma_A^0 \frac{\lambda(k^2)}{\lambda(M_{A_1}^2)} \frac{M_{A_1}^2 + k_0^2}{k^2 + k_0^2} \quad (16)$$

with  $k_0^2$  chosen to satisfy Eq. (15).

We have now completely specified reaction (1) in terms of known constants and the two parameters  $M_A$  and  $g_{A\rho\pi}$ . We can use Eq. (14) to eliminate  $g_{A\rho\pi}$  in favor of  $\Gamma_A^0$ , and so we use  $M_A$  and  $\Gamma_A^0$  as the two parameters we vary to fit the data.<sup>9</sup> In the next section we compare these current-algebra predictions with experiment.

### III. COMPARISON WITH EXPERIMENT

The data on reaction (1) come from experiments done at SLAC<sup>10</sup> and at DESY,<sup>11</sup> which detect the reaction

$$e^+e^- \rightarrow l^+\pi^+\pi^-\pi^+ + \text{undetected neutrals}. \quad (17)$$

The three pions are assumed to be the hadronic decay products<sup>12</sup> of reaction (1), while the lepton is presumably the product of a purely leptonic decay. Each experiment has so far detected about 40 such events, and so the errors are still rather large. The measured branching ratios are

$$\text{SLAC: } B(\tau^\pm \rightarrow \nu_\tau \pi^+ \pi^- \pi^\pm) = 0.060 \pm 0.045 \quad (18)$$

and

$$\text{DESY: } B(\tau^\pm \rightarrow \nu_\tau \pi^+ \pi^- \pi^\pm) = 0.050 \pm 0.015. \quad (18')$$

In the DESY data there is an additional 30% systematic error. The three-pion mass spectra are shown in Figs. 1 and 2. We note that the spectra appear to be rather broad with perhaps some en-

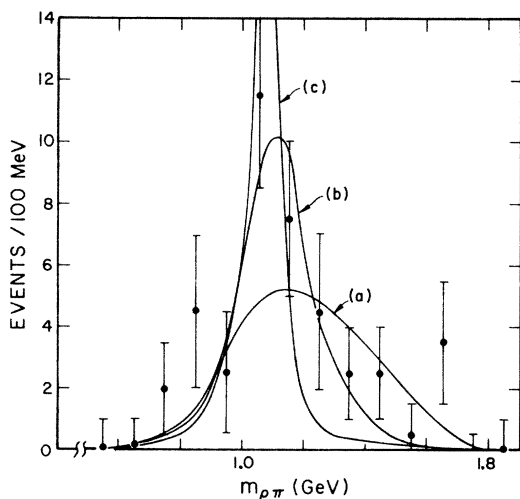


FIG. 1. The SLAC  $\rho^0 \pi^+$  mass spectrum with the following theoretical curves normalized to give the best  $\chi^2$  fit: (a)  $\Gamma_A^0=0$  (no  $A_1$ ),  $\chi^2=10.8$ ; (b)  $\Gamma_A^0=0.27$  GeV,  $M_A=1.15$  GeV,  $\chi^2=9$ ; (c)  $\Gamma_A^0=0.1$  GeV,  $M_A=1.1$  GeV,  $\chi^2=14.9$ .

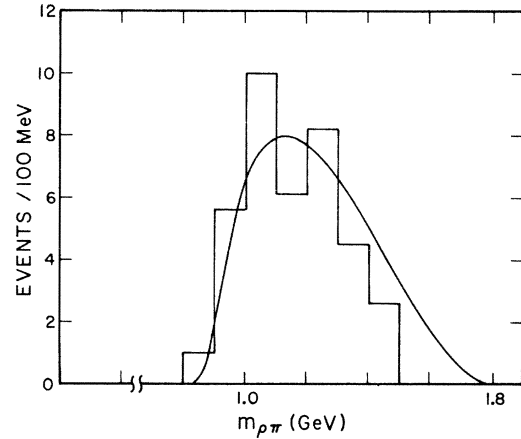


FIG. 2. The DESY  $\rho^0 \pi^+$  mass spectrum along with the theoretical curve for  $\Gamma_A^0=0$ .

hancement in the neighborhood of 1.1 GeV. Owing to the large errors we treat the analyses of the spectrum and the branching ratio separately. We begin by considering the latter.

A convenient way to treat the branching ratio is to consider the relative branching ratio,

$$R = \Gamma(\tau^\pm \rightarrow \nu_\tau \rho_0 \pi^\pm) / \Gamma(\tau \rightarrow \nu_\tau l \nu). \quad (19)$$

The denominator of this fraction is simply

$$\Gamma(\tau \rightarrow \nu_\tau l \nu) = \frac{G_F^2 m_\tau^5}{192 \pi^3}. \quad (20)$$

Combining Eqs. (5) and (20) we find

$$R = \frac{6}{m_\tau^8} I, \quad (21)$$

with

$$I = \int I(k^2) dk^2.$$

The DESY experiments<sup>13</sup> find that  $B(\tau \rightarrow \nu_\tau l \nu) = 0.182 \pm 0.028$ . Combining this number with the SLAC<sup>14</sup> three-pion branching ratio we find

$$R_{\text{exp}} = 0.32 \pm 0.24. \quad (22)$$

Given the experimental value<sup>13</sup>  $m_\tau = 1.807 \pm 0.020$ , Eqs. (21) and (22) put some constraints on  $I$  and hence on  $M_A$  and  $\Gamma_A^0$ .

To see how the rather loose experimental constraints on  $I$  restrict our analysis we plot our theoretical value for  $R$  vs  $\Gamma_A^0$  for  $M_A = 1.1, 1.2,$  and  $1.3$  GeV in Figs. 3–5. The curves for two values of  $\delta$  ( $\delta=0$  and  $0.12$ ) are shown in order to give some idea of the uncertainty in our theoretical predictions. In each of the three  $\delta=0$  curves the value of  $R$  at  $\Gamma_A^0=0$  is the same. This is simply a reflection of the fact that  $\Gamma_A^0=0$  corresponds to

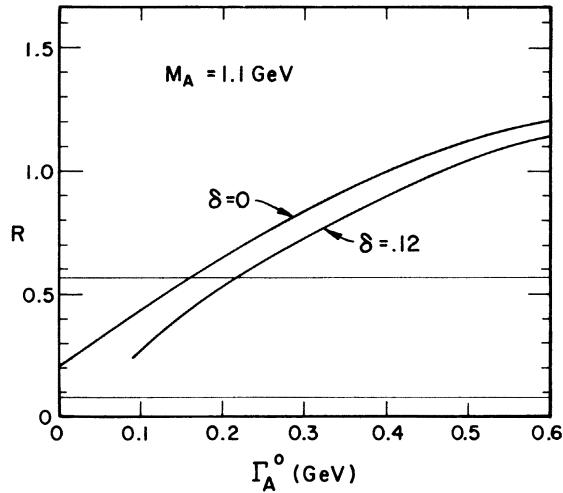


FIG. 3. Graph of  $R$  vs  $\Gamma_A^0$  for  $M_A = 1.1$  GeV with  $\delta = 0$  and  $0.12$ .

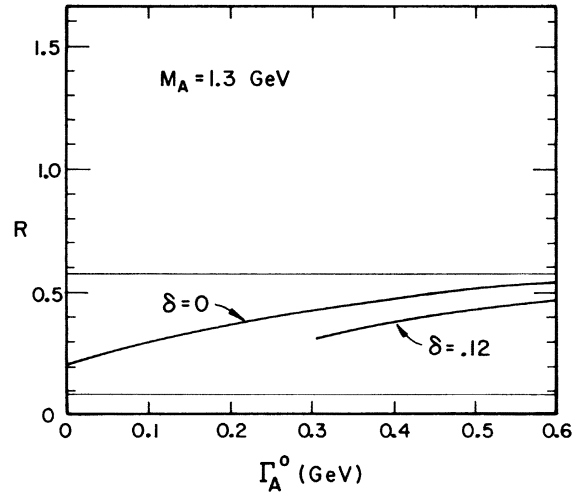


FIG. 5. Graph of  $R$  vs  $\Gamma_A^0$  for  $M_A = 1.3$  GeV with  $\delta = 0$  and  $0.12$ .

our “no- $A_1$ ” case, where the  $A_1$  mass is clearly irrelevant. Superimposed on Figs. 3–5 are the experimental constraints of Eq. (22).

It is clear that the rather wide band of allowed  $R$  values puts restrictions on  $\Gamma_A^0$  which weaken with increasing  $M_A$ . We point out, however, that the no- $A_1$  case ( $\Gamma_A^0 = 0$ ) falls well within the allowed region, and so on the basis of the branching ratio alone we cannot rule out this possibility.

We return now to the question of the  $\rho\pi$  mass distribution. For each pair of values for  $M_A$  and  $\Gamma_A^0$  Eq. (5) predicts a particular spectral shape. Putting aside for the moment the question of the

branching ratio, we can arbitrarily normalize these curves to best fit the data. In Fig. 6 we show the curve for  $\chi^2$  vs.  $\Gamma_A^0$  obtained by using Eq. (5) to fit the SLAC data. The particular curve shown is for  $M_A = 1.1$  GeV and  $\delta = 0$ . The curves for other values of the parameters are similar. The important feature of the curve is that the best fits occur when  $\Gamma_A^0$  is either large or small. Intermediate values ( $50 \text{ MeV} \leq \Gamma_A^0 \leq 150 \text{ MeV}$ ) are not favored. The reason for this behavior is clear. The data show a fairly broad spectrum, and such a spectrum can be realized by either having a broad  $A_1$  or by having the spectrum dominated by the broad no- $A_1$  spectrum (the small- $\Gamma_A^0$  case).

A glance at Fig. 6 would seem to indicate that

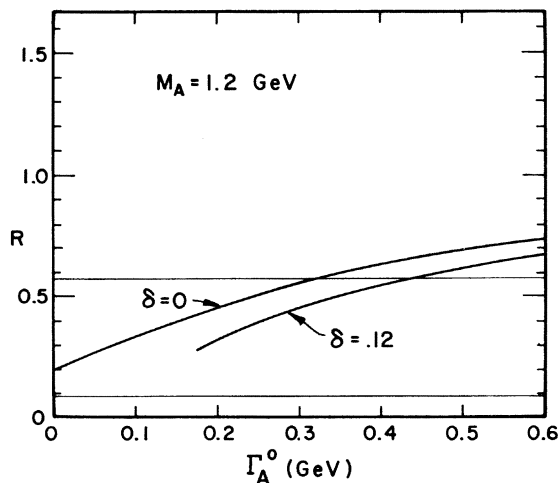


FIG. 4. Graph of  $R$  vs  $\Gamma_A^0$  for  $M_A = 1.2$  GeV with  $\delta = 0$  and  $0.12$ .

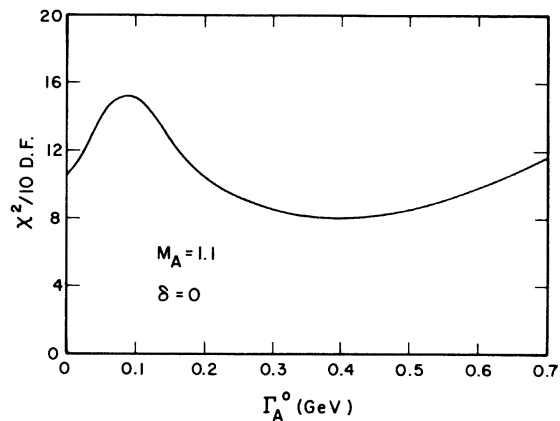


FIG. 6. Graph of  $\chi^2$  vs  $\Gamma_A^0$  for the case  $M_A = 1.1$  GeV,  $\delta = 0$ .

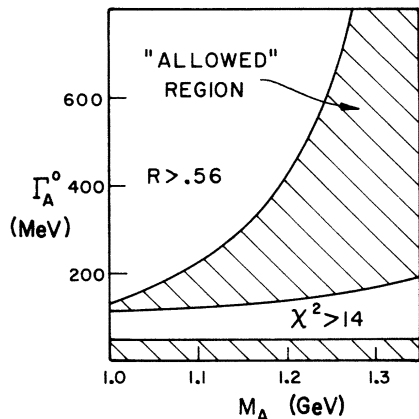


FIG. 7. Graph of the values of  $M_A$  and  $\Gamma_A^0$  allowed by the SLAC data.

$M_A = 1.1$  GeV,  $\Gamma_A^0 = 400$  MeV is a very good fit. This is not the case, however, because  $\Gamma_A^0 \approx 400$  MeV gives a very bad fit to  $R$ . Both the shape and the branching ratio must be fitted simultaneously. A summary of our findings with these dual constraints is shown as an "allowed" region in  $M_A - \Gamma_A^0$  space given in Fig. 7. The upper curved line is the constraint we get from the branching ratio, i.e., Eq. (22). The second forbidden region is determined by the constraint  $\chi^2/10 \text{ DF} > 14$ .  $\chi^2$  of 14 for 10 degrees of freedom corresponds to a confidence level of 0.15.

The large area of the allowed region in Fig. 7 is a reflection of the large statistical and systematic errors in the experiments. Indeed, the constraints chosen to define the allowed region are somewhat arbitrary and should not be taken as ironclad. However, the constraints do define regions of "good" or "bad" fits. So that the reader can judge for himself, we have included in Fig. 1 two good fits ( $\Gamma_A^0 = 0$ ;  $\Gamma_A^0 = 0.27$  GeV,  $M_A = 1.15$  GeV,  $\delta = 0.12$ ) and one bad fit ( $\Gamma_A^0 = 0.1$  GeV,  $M_A = 1.1$ ,  $\delta = 0$ ) normalized to fit the data. We have also included the  $\Gamma_A^0 = 0$  curve<sup>15</sup> with the DESY data of Fig. 2. We once more point out that the data are entirely consistent with the no- $A_1$  case in addition to a wide range of parametrizations for a strongly coupled  $A_1$ . However, a glance at Figs. 3–5 shows that a modest reduction in the error in the branching-ratio measurement would begin to decrease this range considerably.

#### IV. DISCUSSION

The major results of our analysis are summarized in Fig. 7. The allowed region for small or zero  $A_1$  width leads to the clear conclusion that

the available data for  $\tau \rightarrow \nu_\tau \rho \pi$  gives no evidence for the existence of the  $A_1$ . We emphasize that our model with no  $A_1$  predicts both an acceptable mass distribution and rate for this decay mode.

This, of course, does not rule out the  $A_1$ , which we believe does exist. The evidence for the quark-antiquark structure of mesons has become increasingly convincing. The observation of the  $\chi$  multiplet in charmonium almost certainly confirms the presence of a charmonium analog to the  $A_1$ . Since for light-quark systems the  $^3P_2$  ( $A_2, f_0$ ) and  $^1P_1$  ( $B$ ) states are well established and almost degenerate, it is hard to imagine a dynamical mechanism suppressing the  $^3P_1$  ( $A_1$ ) state. For example, a recent relativistic light-quark model for mesons<sup>16</sup> finds an  $A_1$  appearing as a chiral partner to the  $\rho$  with a mass in the 1-GeV region.

Reaction (1) still remains the cleanest known way to establish the  $A_1$  and fix its parameters. Our results show, however, that more precise data will be required in order to do this. That this is so follows from our second major conclusion: unless the relative branching ratio  $R$  is larger than present limits indicate, the  $A_1$  cannot completely dominate this  $\tau$  decay mode.

The possibility remains, of course, that the  $A_1$  exists but does not conform to our predictions. Most current-algebra models predict  $A_1$  widths of less than 200 MeV for  $M_A \approx 1.1$  GeV. The  $SU(6)_w$  approach,<sup>17</sup> which is quite successful, also yields similar predictions. From Fig. 7 we see that this range of parameters is not completely ruled out but has become less likely. In addition, we note that the recent backward-production experiment alluded to in the Introduction<sup>4</sup> gives values for  $M_A$  and  $\Gamma_A^0$  which lie somewhat outside our allowed region. Thus, we are led to consider where our approach might break down.

First, we remind the reader that current-algebra calculations are typically good only to about 20%, and so we should probably allow some leeway in fitting the parameters. In addition, our model makes certain assumptions about the dominance of the vertex function by low-lying mesons which may or may not be correct. In particular we have assumed that only  $F_0$  needs a subtraction, so that there is only one subtraction constant,  $C_0$ , in Eqs. (2). If  $F_+$  and/or  $F_-$  also have significant high-mass contributions, then additional constants may be needed, and one or both of our sum rules, Eqs. (10) and (12), may be invalidated. If that is the case, then the predictive power of our model is greatly reduced.

To end on a more positive note we point out that if our predictions do fit the data then we will know all the important physical parameters of the  $A_1$ ,

including  $M_A$ ,  $\Gamma_A^0$ , and  $F_A$ . On the other hand, even if our particular model is not successful we can turn our arguments around and learn something about the higher-mass contributions to the vector and axial-vector currents. We emphasize again that in order to do this good measurements of both the mass spectrum and the branching ratio are required.

## ACKNOWLEDGMENTS

We would like to thank J. L. Rosner for helpful conversations concerning the  $SU(6)_w$  approach and H. Joos for providing information on the DESY data. This work was supported in part by the U. S. Department of Energy under Contract No. E(11-1)-1764.

<sup>1</sup>Y. S. Tsai, Phys. Rev. D 4, 2821 (1971); H. B. Thacker and J. J. Sakurai, Phys. Lett. 36B, 103 (1971).

<sup>2</sup>A discussion of the problem and many references are in a paper by H. E. Haber and G. L. Kane, Nucl. Phys. B129, 429 (1977).

<sup>3</sup>M. G. Bowler, M. A. V. Game, I. J. R. Aitchison, and J. B. Dainton, Nucl. Phys. B97, 227 (1975); R. S. Longacre and R. Aaron, Phys. Rev. Lett. 26, 1509 (1977); J. L. Basdevant and E. L. Berger, Phys. Rev. D 16, 657 (1977). Basdevant and Berger have also recently analyzed reaction (1) as an  $A_1$ -dominated process, using the masses and widths obtained in their work on diffractively produced  $A_1$ 's cited above. They find that their lowest-mass fit to hadron production data ( $M_A \approx 1200$  MeV,  $\Gamma_A \approx 400$  MeV) is consistent with existing data on  $\tau$  decay. [J. L. Basdevant and E. L. Berger, Phys. Rev. Lett. 40, 994 (1978)].

*Note added.* While completing the manuscript for this paper we received two relevant reports. One, by R. Aaron, H. Goldberg, and R. S. Longacre [North-eastern Report No. 2350, 1978 (unpublished)] also finds our no- $A_1$  current-algebra result but seems to disagree with our numerical results for reasons we do not understand. The other report is by T. N. Pham, C. Roiesnel, and Tran N. Truong [Ecole Polytechnique Report No. AA294.9378, 1978 (unpublished)]. The latter paper applies the soft-pion limit to an  $F_0(k^2)$  dominated by the  $A_1$  pole without a subtraction term and hence without background. This implies a subtraction for  $F$ , instead. Theirs is an unconventional approach, therefore, but which cannot be ruled out *a priori*, although applying these same assumptions to  $\langle \pi | V_\mu | A_1 \rangle$  would lead to difficulties. Nevertheless, they find acceptable fits to the spectrum and branching ratio with  $M_A = 1.1$  GeV and  $\Gamma_A > 250$  MeV. They also obtain a no- $A_1$  branching ratio which agrees with ours if we make their approximations.

<sup>4</sup>Ph. Gavillet *et al.*, Phys. Lett. 69B, 119 (1977). A backward-produced  $(3\pi)^-$  peak in  $\pi^-p$  collisions at 9 and 12 GeV has also been reported at the 1977 Meson Spectroscopy Conference at Budapest, private communication. The bump is fitted with an  $A_1$ :  $M_A \approx 1050$  MeV,  $\Gamma_A \approx 200$  MeV.

<sup>5</sup>D. A. Geffen, Phys. Rev. Lett. 19, 770 (1967). Other references can be found in the review article on effec-

tive Lagrangians by S. Casiorowicz and D. A. Geffen, Rev. Mod. Phys. 41, 531 (1969). The reader should note that in the Lagrangian approach discussed in the latter reference, the  $A\rho\pi$  coupling-constant sum rules are restricted to the special case  $F_A = F_\rho$  which tends to follow naturally from simple field-algebra models for  $SU(2) \times SU(2)$ .

<sup>6</sup>In Eq. (2) we take the universal form for spin- $\frac{1}{2}$  lepton weak-interaction couplings. Since we are dealing with branching ratios, we actually need only assume that the  $\tau$  and  $\nu_\tau$  are spin- $\frac{1}{2}$  leptons which couple to the same charged intermediate boson  $W^\pm$  as do the electron and muon leptons. We use Eq. (2) for simplicity.

<sup>7</sup>Particle Data Group, Rev. Mod. Phys. 48, S1 (1976).

<sup>8</sup>As an example of a problem of this type see G. Gounaris, and J. J. Sakurai, Phys. Rev. Lett. 21, 244 (1968).

<sup>9</sup>We also take into account the finite width of the  $\rho$  meson. Equations (5) and (14) are smeared out as a function of the  $\rho$  mass using a technique similar to the one we used to treat the  $A_1$  width.

<sup>10</sup>J. A. Jaros *et al.*, Phys. Rev. Lett. 40, 1120 (1978).

<sup>11</sup>Conference on Particle Physics at Vanderbilt University, 1978; G. Alexander *et al.*, Phys. Lett. 73B, 99 (1978).

<sup>12</sup>The three-pion distribution in Ref. 11 is consistent with being entirely due to the decay of the  $\rho\pi$  final state.

<sup>13</sup>PLUTO Collaboration, DESY Report No. 77/81, 1977 (unpublished).

<sup>14</sup>We use the SLAC (See Ref. 10) value for the branching ratio for two reasons: firstly, to be consistent, since we use their measurement of the  $\rho\pi$  spectrum in our  $\chi^2$  analysis and, secondly, because the DESY measurement also contains a 30% systematic error which is difficult to take into account. In any case, it is advisable to treat these first relatively few events conservatively.

<sup>15</sup>The  $\Gamma_A^0 = 0$  curves for SLAC (Fig. 1) and DESY (Fig. 2) differ slightly because there is a  $\rho$ -mass cut ( $0.70$  GeV  $\leq m_{\pi^+\pi^-} \leq 0.84$  GeV) on the DESY data but not on the SLAC data.

<sup>16</sup>D. A. Geffen and H. Suura, Phys. Rev. D 16, 3305 (1977).

<sup>17</sup>J. L. Rosner, Phys. Rep. 11C, 189 (1974).

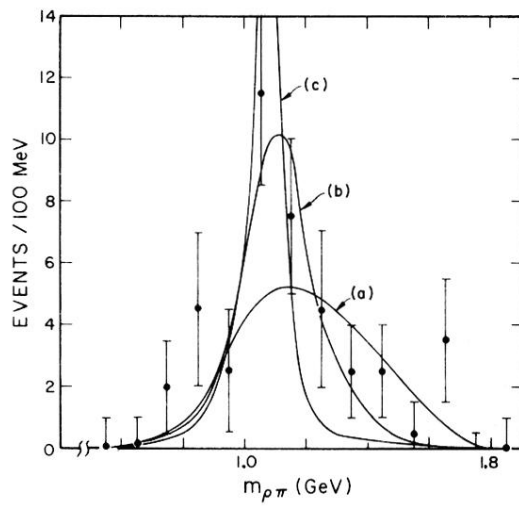


FIG. 1. The SLAC  $\rho^0\pi^+$  mass spectrum with the following theoretical curves normalized to give the best  $\chi^2$  fit: (a)  $\Gamma_A^0=0$  (no  $A_1$ ),  $\chi^2=10.8$ ; (b)  $\Gamma_A^0=0.27$  GeV,  $M_A=1.15$  GeV,  $\chi^2=9$ ; (c)  $\Gamma_A^0=0.1$  GeV,  $M_A=1.1$  GeV,  $\chi^2=14.9$ .



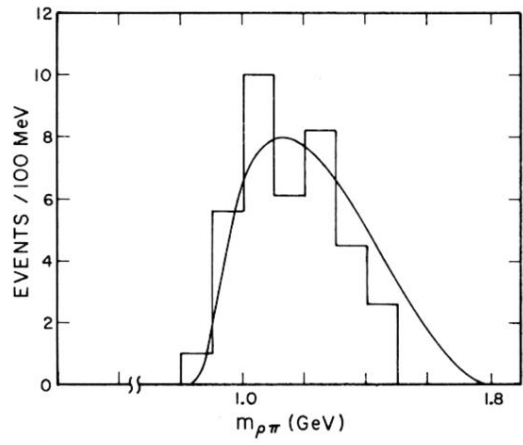


FIG. 2. The DESY  $\rho^0 \pi^+$  mass spectrum along with the theoretical curve for  $\Gamma_A^0 = 0$ .

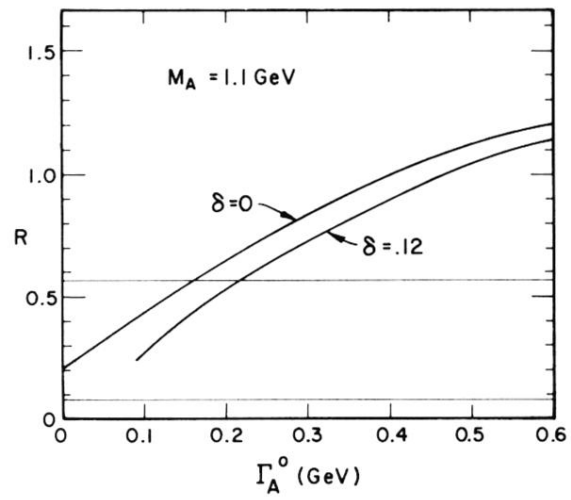


FIG. 3. Graph of  $R$  vs  $\Gamma_A^0$  for  $M_A = 1.1$  GeV with  $\delta = 0$  and 0.12.

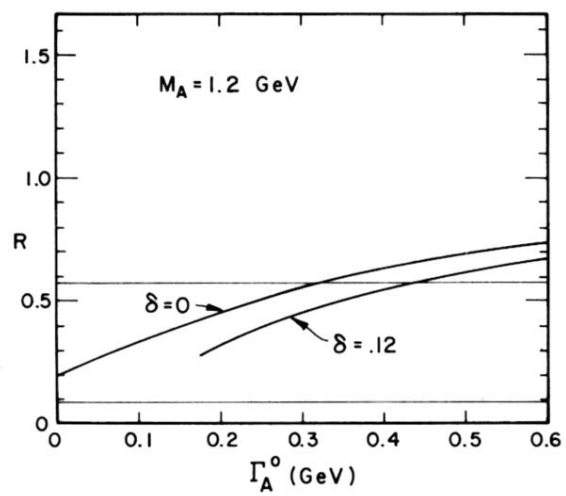


FIG. 4. Graph of  $R$  vs  $\Gamma_A^0$  for  $M_A = 1.2$  GeV with  $\delta = 0$  and 0.12.

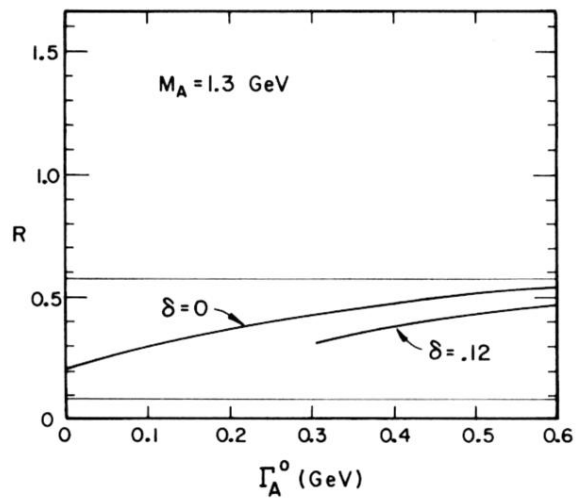


FIG. 5. Graph of  $R$  vs  $\Gamma_A^0$  for  $M_A = 1.3$  GeV with  $\delta = 0$  and 0.12.

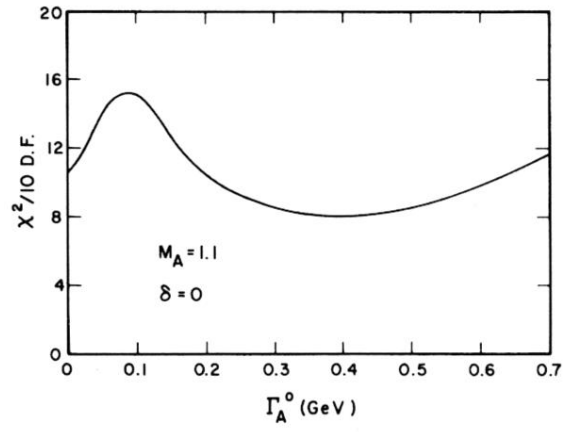


FIG. 6. Graph of  $\chi^2$  vs  $\Gamma_A^0$  for the case  $M_A = 1.1$  GeV,  $\delta = 0$ .

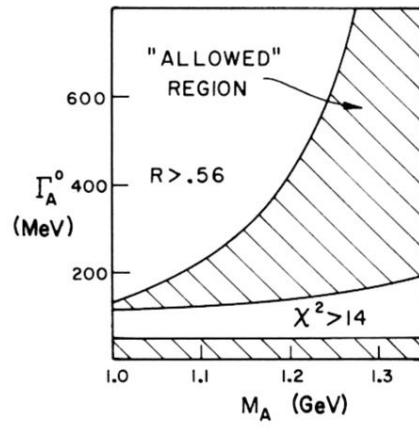


FIG. 7. Graph of the values of  $M_A$  and  $\Gamma_A^0$  allowed by the SLAC data.